Supporting Information

Micron-Sized Water Droplets Induce Spontaneous Reduction

Jae Kyoo Lee[1], Devleena Samanta[1†], Hong Gil Nam[2,3*], Richard N. Zare[1*]

[1]Department of Chemistry, Stanford University, Stanford, CA 94305, USA.

[2]Center for Plant Aging Research, Institute for Basic Science, Daegu 42988, Republic of Korea.

[3]Department of New Biology, DGIST, Daegu 42988, Republic of Korea.

[†]Present Address: Department of Chemistry and International Institute for Nanotechnology, Northwestern University, 2145 Sheridan Road, Evanston, Illinois 60208, USA

*Correspondence to: zare@stanford.edu and nam@dgist.ac.kr

Table of Contents

Materials and Methods

Chemicals

Pyruvate, lactate, lipoic acid, dihydrolipoic acid, cystine, cysteine, fumarate, succinate, acetophenone, and redox dye resazurin were purchased from Sigma-Aldrich (St. Louis, MO). HPLC grade water were purchased from Fisher Scientific (Nepean, ON, Canada). Resazurin was purchased from Thermo Scientific (Lafayette, CO).

Generation of microdroplets and mass spectrometric analysis

Microdroplets were generated by spraying a solution containing molecules with a high pressure of dry nebulizing N_2 gas at 120 psi. The solution was injected into a silica capillary (250 μm inner diameter and 350 μm outer diameter) using a syringe pump (Harvard Apparatus) at 10 μl/min flow rate. Thermo Scientific LTQ Orbitrap XL Hybrid Ion Trap-Orbitrap mass spectrometer was used for mass spectrometric analysis of the reaction products in microdroplets. No voltage was applied to the solution. The heated capillary inlet to the mass spectrometer was maintained at approximately 275 °C. The capillary and tube lens voltages were set as - 44 and -60 V. Tandem mass spectrometric analysis was performed to determine molecular identities of reduced or oxidized molecular species. Collision-induced dissociation (CID) mode of the LTQ Orbitrap XL Hybrid Ion Trap-Orbitrap mass spectrometer was used for the analysis.

Tandem mass spectrometric analysis

The identification of the observed reduced or oxidized molecular species was carried out by tandem mass spectrometry using collision-induced dissociation (CID). Fragmentation patterns between original molecules and reduced/oxidized molecules were compared to confirm the identities of the observed molecules. The mass spectra of the CID analysis are presented in Figure S2-5.

Characterization

Several characterizations were made to further understand the nature of the spontaneous reduction. The kinetics of pyruvate reduction was measured by varying the traveling distance of stream of microdroplets between the spray source and the mass spectrometer inlet. A linear micrometer translation stage was used to control the distance. The dependence of the concentration of pyruvate on the reduction efficiency was measured by spraying pyruvate solutions with different concentration from 1 nM to 10 mM. The dependence of the size of microdroplets on the reduction efficiency of pyruvate was assessed by spraying 10 μM pyruvate solution in different sizes of microdroplets. The size was controlled by adjusting the syringe pump pressure or the pressure of the nebulizing gas.

The heated capillary inlet to the mass spectrometer was maintained at approximately 275 °C. The capillary and tube lens voltages were set as +44 and +60 V. To detect hydroxyl radical formation in microdroplets, we sprayed microdroplets containing 10-μM salicylic acid with or without 10-nM pyruvate. This measurement was carried out in negative mode with capillary and tube lens voltages set as -44 and -60 V.

Fluorescence imaging of redox dye in microdroplets
Solution containing the reduction-sensitive dye, resazurin, at 100 nM concentration was prepared in H_2O. This solution was sprayed on pre-cleaned glass coverslips, which were mounted on a confocal microscope. A confocal microscope (Leica TCS SP8) with white light laser was used for the imaging. The confocal microscope was adjusted in order to achieve optical section thickness approximately 0.5 μm. The excitation/emission filters for resazurin are 570/595-630 nm. The exposure time to the excitation laser was minimized to prevent photobleaching of the dye. The glass slide mounted on a microscope stage was enclosed in a humidified chamber to retard evaporation of microdroplets.

NMR analysis
^{1}H NMR spectra were acquired at 300 MHz on a Varian Inova-300 NMR spectrometer (Palo Alto, CA, USA). Standard samples of pyruvate and lactate were prepared by dissolving them in D_2O at 100 μM concentration. The collected microdroplet solution was prepared by collecting sprayed microdroplet containing 100-μM pyruvate in D_2O using a glass vial with silicone rubber cap. The collection bottles were seal except a spray source to minimize evaporation during nebulization. ^{1}H NMR (300 MHz, D_2O) δ 4.84, 2.49 (CH_3, m), 1.61, 1.28 (CH_3, d).

Organic Redox Reactions in Microdroplets
Acetophenone (Sigma-Aldrich) was dissolved in water at 10-μm concentration. The solution was sprayed to form microdroplets which entered the inlet of a mass spectrometer (Thermo Scientific LTQ Orbitrap XL Hybrid Ion Trap-Orbitrap). Mass spectra of reactants and products in microdroplets were recorded. The estimated duration of the reaction was calculated based on the measurement at a traveling distance of 1.5 cm between the spray source and the mass spectrometer inlet.

Calculation of Redox Efficiency

The ratio of relative concentration between oxidized and reduced species was calculated as following formula:

$$\frac{E_{ox}}{E_{red}} = R \tag{1}$$

$$I = C \times E \tag{2}$$

where I denotes intensity, C concentration, E ionization efficiency, and R ratio of ionization efficiency of oxidized form over reduced form:

$$\frac{C_{red}}{C_{ox}} = \frac{I_{red} \big/ E_{red}}{I_{ox} \big/ E_{ox}} = \frac{I_{red}}{I_{ox}} \cdot \frac{E_{ox}}{E_{red}} = \frac{I_{red}}{I_{ox}} \cdot R \tag{3}$$

$$\frac{C_{red}}{C_{ox} + C_{red}} = \frac{I_{red} \big/ E_{red}}{I_{ox} \big/ E_{ox} + I_{red} \big/ E_{red}} = \frac{I_{red} \cdot R}{I_{ox} + I_{red} \cdot R} \tag{4}$$

$$\text{Reduction efficiency (\%)} = \frac{I_{red} \cdot R}{I_{ox} + I_{red} \cdot R} \times 100 \tag{5}$$

We measured the relative ionization efficiency, R, by spraying microdroplets containing both original compounds and reduced compounds with equal concentration at 10 μM. The measured R values for lactate/pyruvate, dihydrolipoic acid/lipoic acid, succinate/fumarate, and oxaloacetate/malate were 0.58, 0.39, 2.00, and 0.24, respectively.

Discussion about Possible Mechanisms for Reduction in Water Microdroplets

From what has been presented, it seems well established that sprayed aqueous microdroplets are capable of causing spontaneous reduction. For reduction to occur there needs to be a source that provides electrons. At present, we have been unable to establish conclusively the mechanism for the reduction processes that we have observed, but several possibilities are suggested. One involves electrification on contact of the water with silica tubing or with air; another involves friction that causes triboelectrification; a third possibility is charging caused by charge separation during droplet fission; and a fourth possibility is donation of electrons from OH^- at or near the surface of the microdroplet to water to form hydrated electrons. As will be explained, we favor the last possibility.

We first examine whether reduction originates from charge transfer between the silica capillary and the water inside the capillary. It is well known that contact between two different materials can lead to contact electrification.[1] We replaced the silica capillary with a stainless steel capillary which was grounded (0 V). We also applied a DC voltage to the metal capillary ranging between -29 V and +29 V, which clearly exceeds the reduction potential of pyruvate.[2] Figure S10 shows the experiment setup (Figure S15a) and a mass spectrum (Figure S15b) of 1 μM pyruvate solution in the microdroplet spray with different applied voltages. We observed almost no influence of applied voltage on the reduction efficiency. We conclude that the reduction is not likely occurring at the interface between capillary and water caused by contact electrification.

We have also examined whether the reduction occurs in the charged microdroplets as in electrospray ionization (ESI) mass spectrometry. We varied polarity and intensity of the applied potential and measured the reduction efficiency of ESI droplets containing 10-μM pyruvate (Figure S16). Positive potential at 500 V or higher was effective in suppressing reduction; whereas, negative potential promoted the reduction reaction. However, the same reduction reaction efficiency increased to above 90% by lowering reactant concentration and to approximately 10 % by generating smaller microdroplets, which indicates that the redox reaction originate from the properties of microdroplets.

Another possibility is streaming electrification. For example, this phenomenon has been reported by Crooks and coworkers who showed that solution flow can generate streaming potentials on the order of volts.[3] We examined this possibility by measuring reduction efficiency of 10 μM pyruvate with different capillary lengths and observed almost no difference in the efficiency (Figure S17). Moreover, the lack of the change of reduction efficiency using a grounded stainless steel capillary suggests that triboelectrification does not occur inside the capillary, although we cannot rule out its effect for the travel of the water microdroplet in air.

Another cause might be charge separation during droplet fission or evaporation.[4] Previously, we reported that aqueous microdroplets maintain their sizes with minimum evaporation up to approximately 130 μs of microdroplet traveling time.[5-6] Moreover, asymmetric fission has been measured to occur on a longer timescale.[7] Nevertheless, we still observed a rapid reduction of molecules in microdroplets (Figure 2a) in less than 130 μs, indicating that droplet fission or evaporation might not be a major cause of reduction.

The last possible mechanism we have considered is the donation of electrons from hydroxide anions near the water-air interface. We do not know exactly where such a transfer might occur. Further work is needed to establish whether the observed reactions of molecules in the pneumatically driven microdroplets involve condensed phase reactions in the microdroplets, gas-phase reactions near the air-water interface, or action at and near the interface, or some combination thereof. The energy required to remove an electron form OH^- in the liquid phase is about 9.2 eV.[8] However, ionization energy and oxidation potential at the water-air interface can be lower than in bulk;[9] thus, t the water-air interface lowers the energy barrier for causing the transfer of electron from OH^- to species to result in reduction.

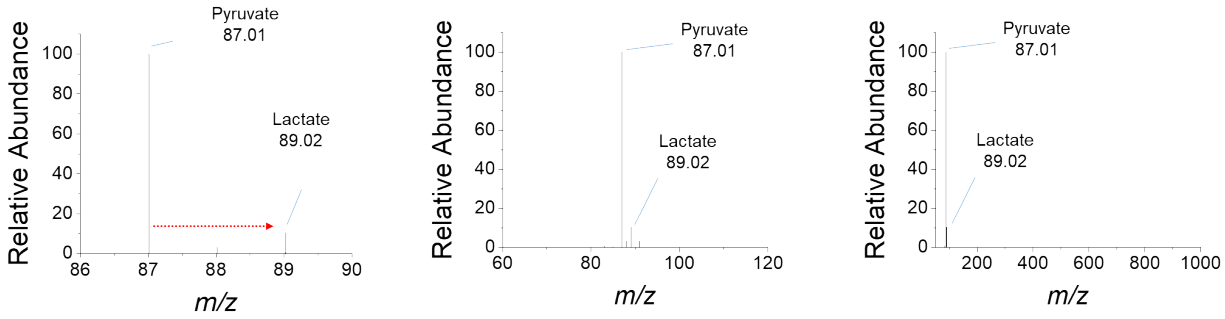

Figure S1. Mass Spectra of 10-µM pyruvate with different *m/z* ranges.

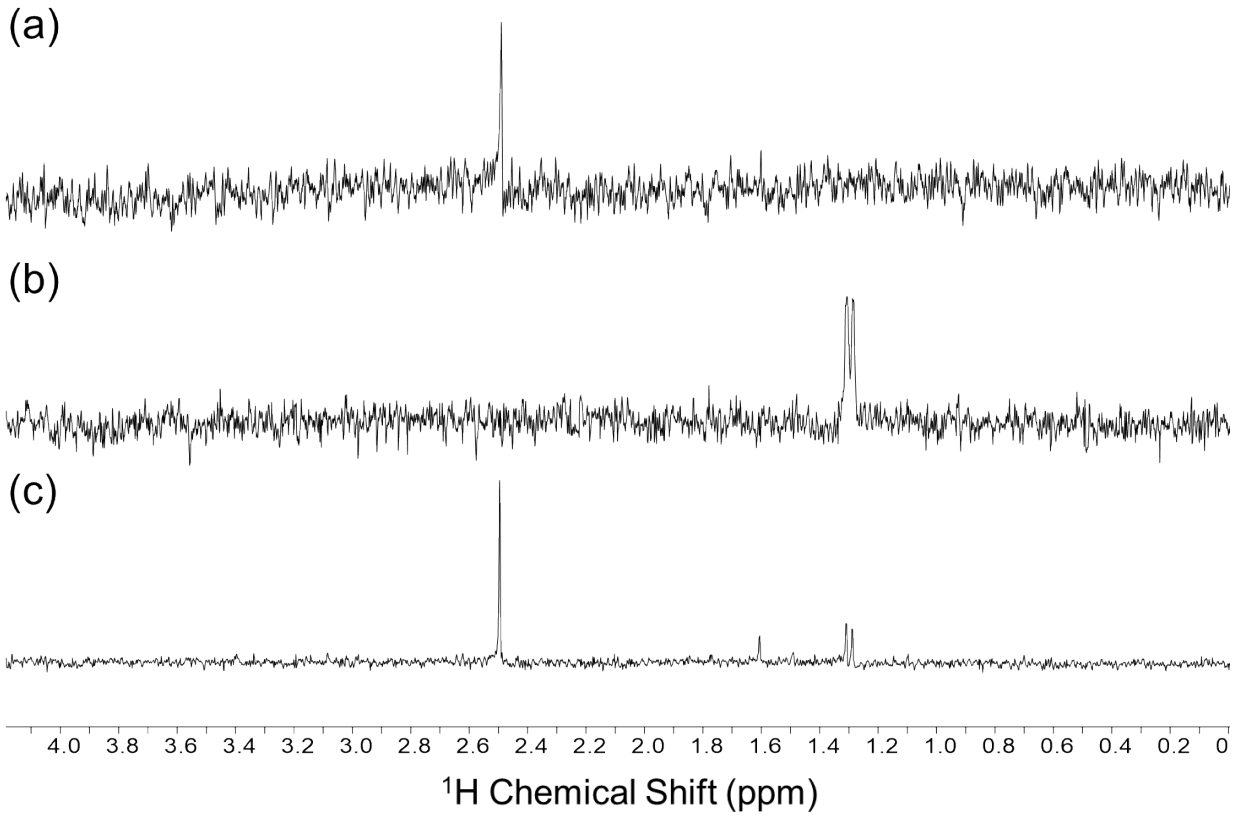

Figure S2. ^{1}H NMR spectra of (a) 100 μM pyruvate, (b) 100 μM lactate, and (c) collected microdroplets containing 100 μM pyruvate in D_2O. The resonance of CH_3 from pyruvate at 2.49 ppm as a singlet and from lactate at 1.30 ppm as a double enables the identification between the original and the reduced compounds. The solution with a low concentration at 100 μM was used because the efficiency of reduction in microdroplet becomes higher at lower concentration. The presence of the doublet resonance at 1.30 ppm in collected microdroplet solution shows a part of the pyruvate molecules converted into reduced species, lactate. A quartet at around 4 ppm is expected, but could not be observed possibly due to the low concentration of pyruvate and consequently the low signal intensity below the detection limit of NMR.

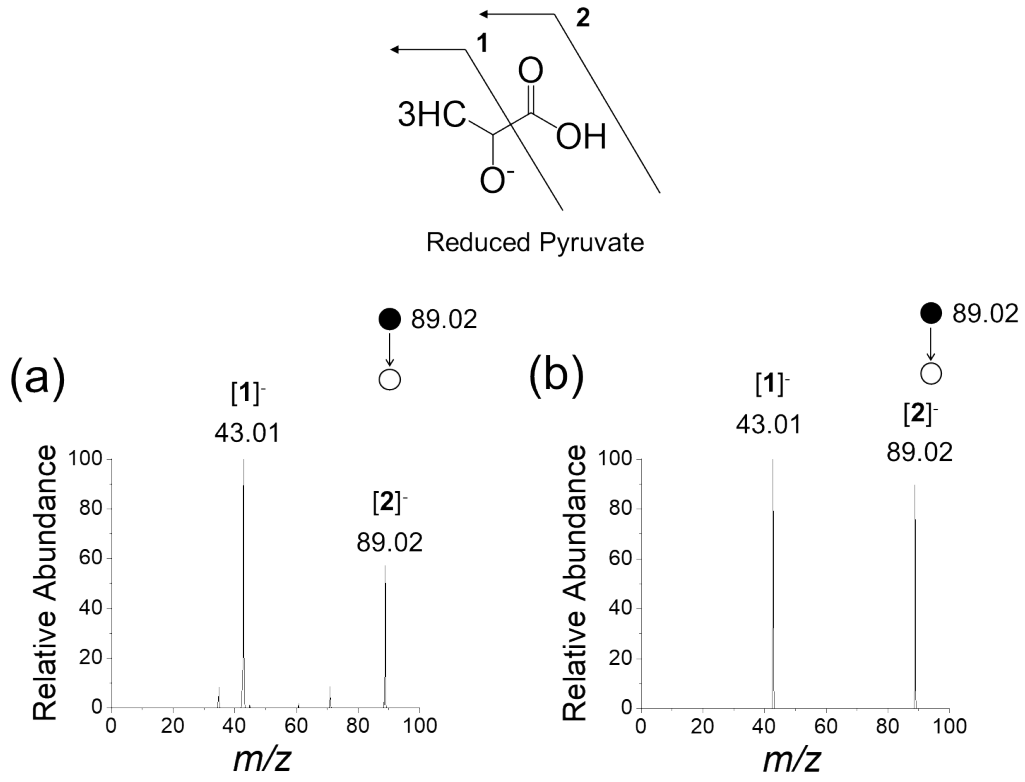

Figure S3. Tandem MS analysis of (a) reduced pyruvate observed in microdroplets and (b) standard sample of lactate.

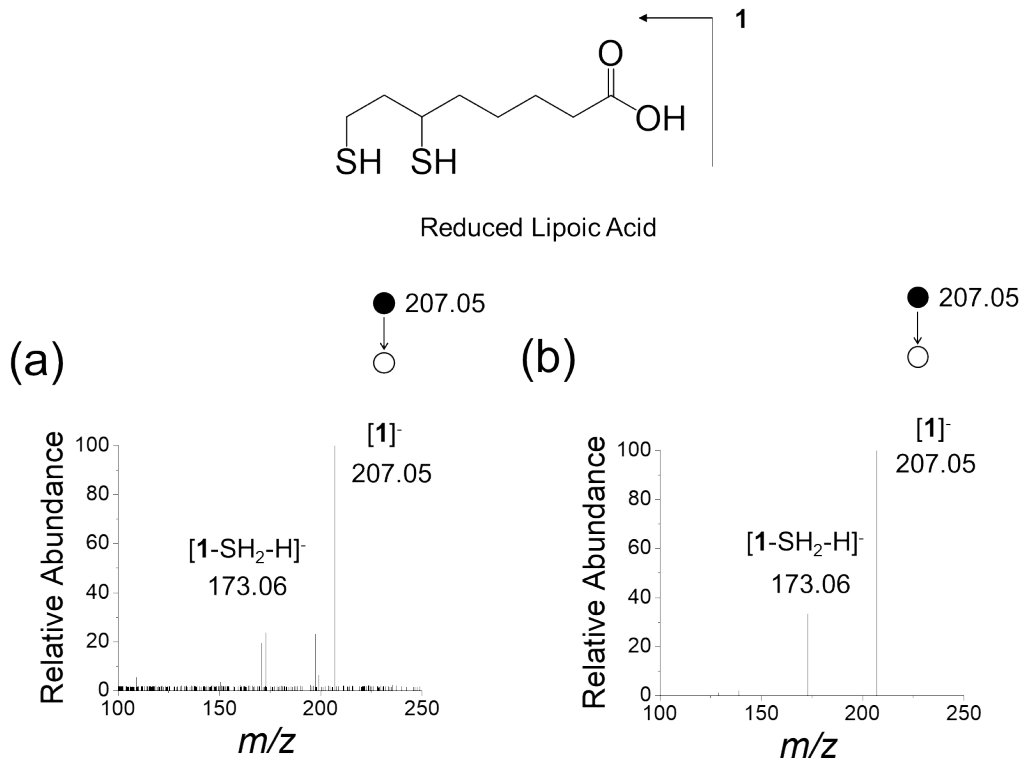

Figure S4. Tandem MS analysis of (a) reduced lipoic acid observed in microdroplets and (b) standard sample of dihydrolipoic acid.

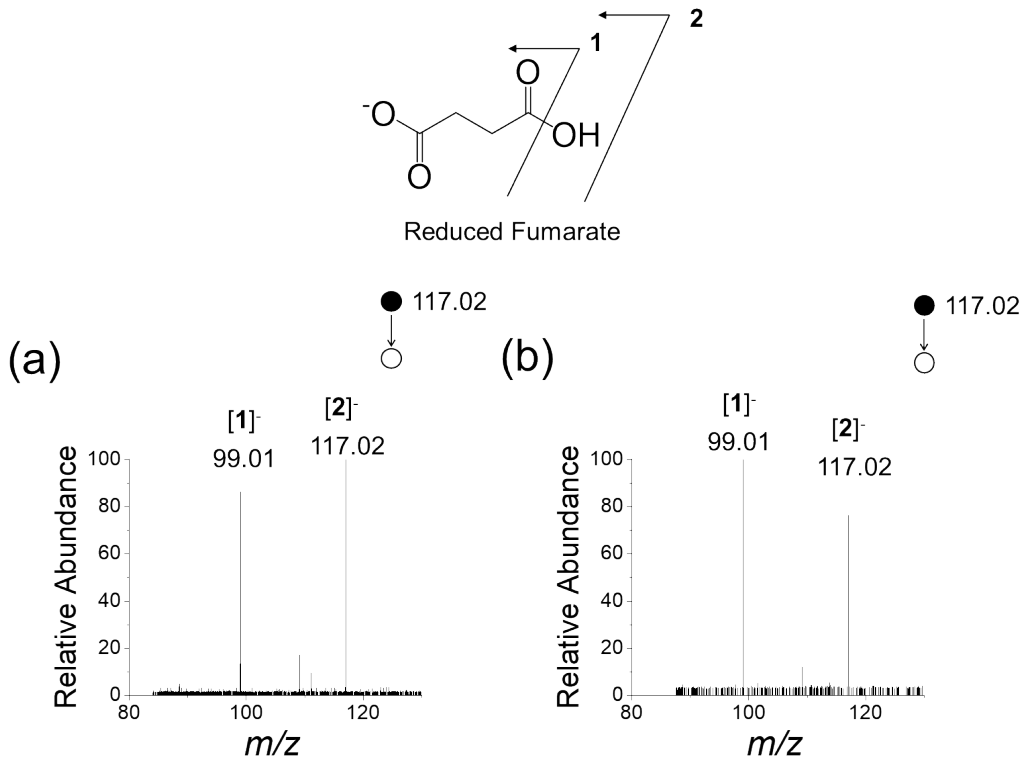

Figure S5. Tandem MS analysis of (a) reduced fumarate observed in microdroplets and (b) standard sample of succinate.

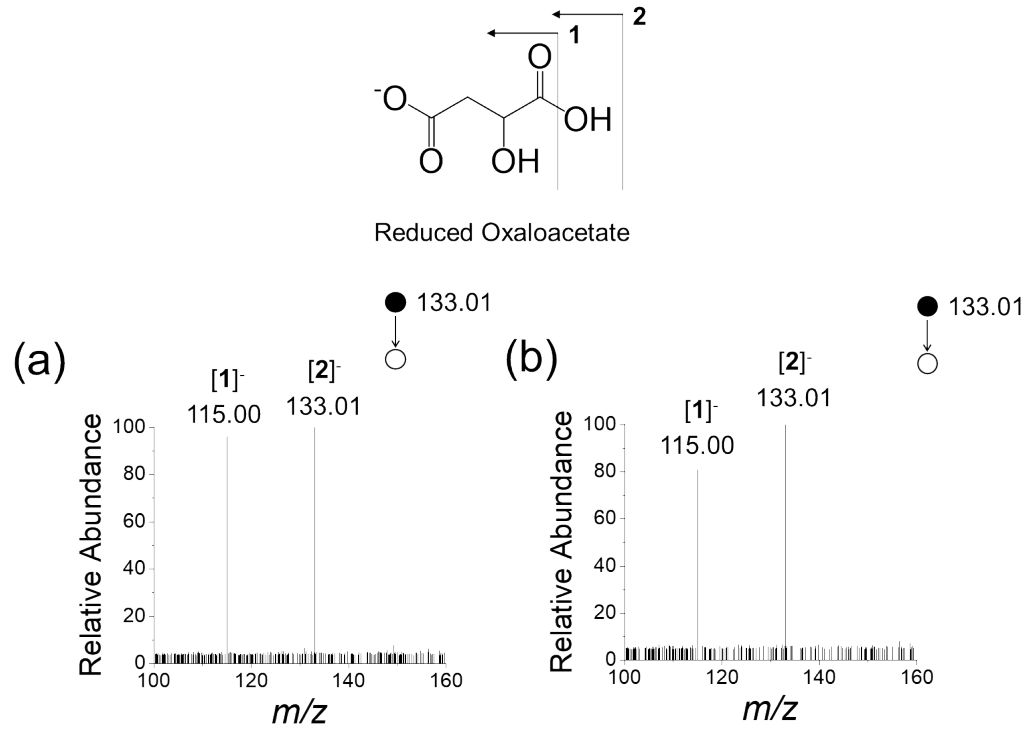

Figure S6. Tandem MS analysis of (a) reduced oxaloacetate observed in microdroplets and (b) standard sample of malate.

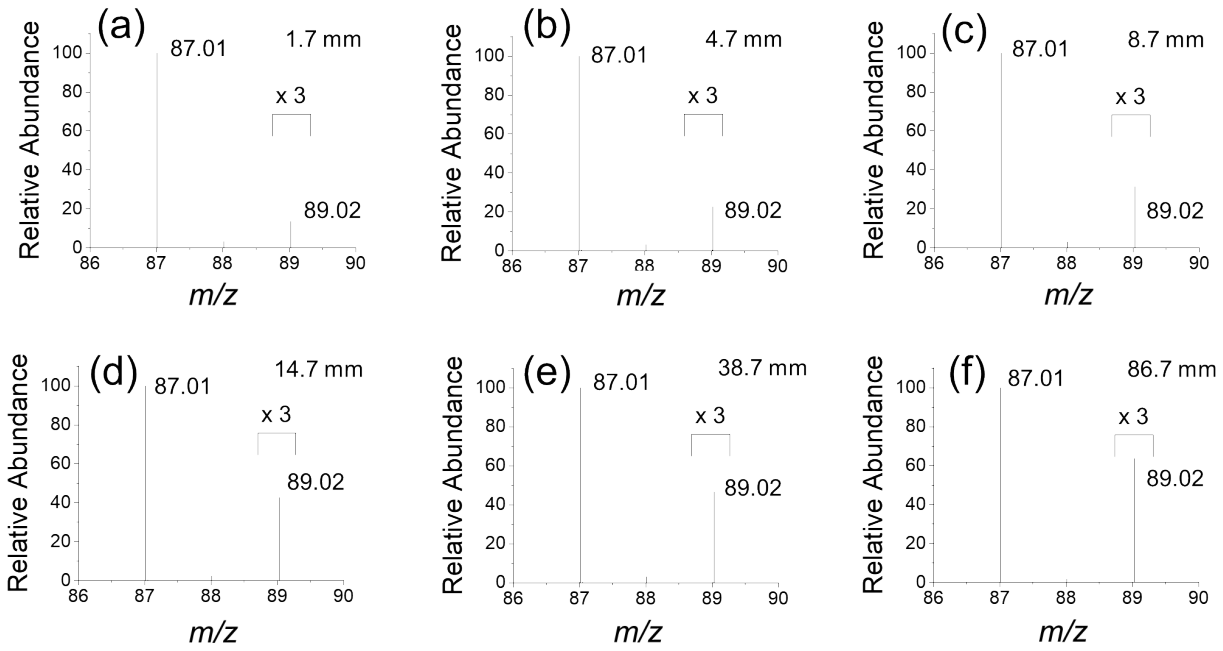

Figure S7. Mass spectra of 10-μM pyruvate in microdroplets at different traveling distances. (a) 1.7 mm, (b) 4.7 mm, (c) 8.7 mm, (d)14.7 mm, (e) 38.7 mm, and (f) 86.7 mm.

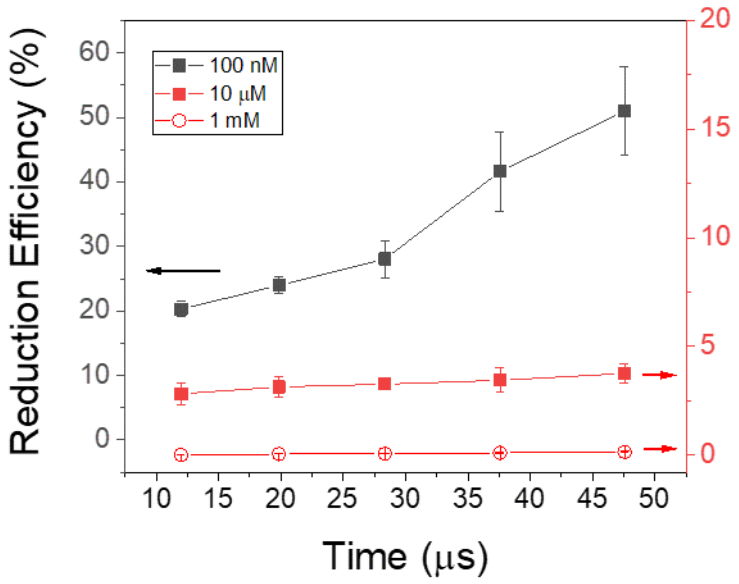

Figure S8. Kinetics of the reduction reaction of 100-nM, 10-μM, and 1-mM pyruvate. The error bars represent one standard deviation from three independent measurements.

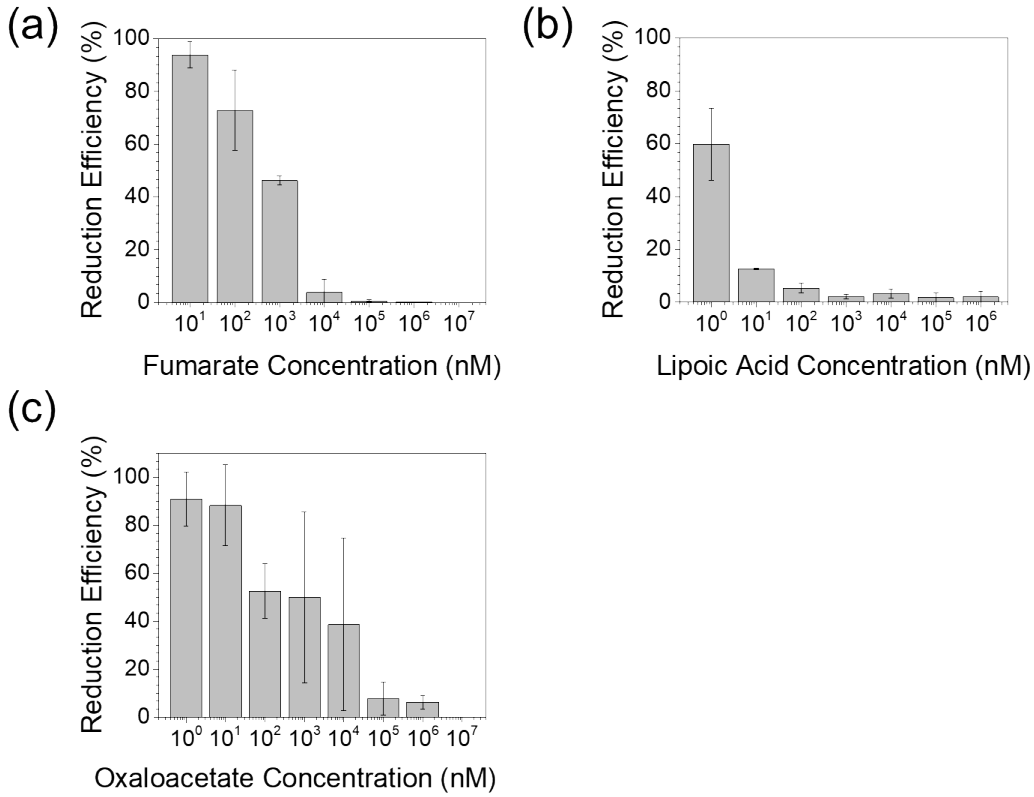

Figure S9. Concentration dependence of reduction efficiency for (a) fumarate, (b) lipoic acid, and (c) oxaloacetate. The error bars represent one standard deviation from three independent measurements.

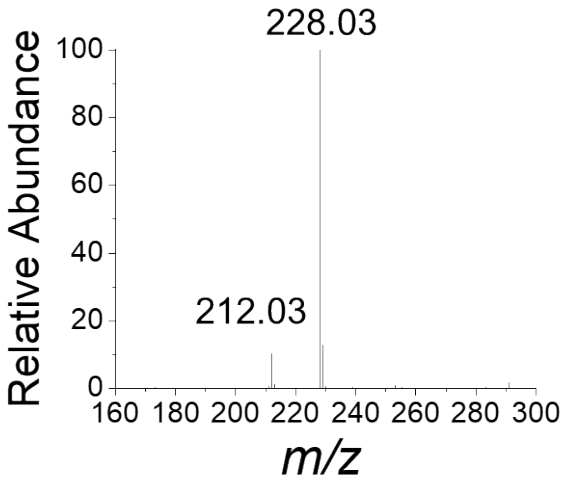

Figure S10. Mass spectrum of sprayed aqueous microdroplets containing 1-μM resazurin. The *m/z* peaks at 228.03 and 212.03 correspond to deprotonated resazurin and resorufin, the reduced form of resazurin, respectively.

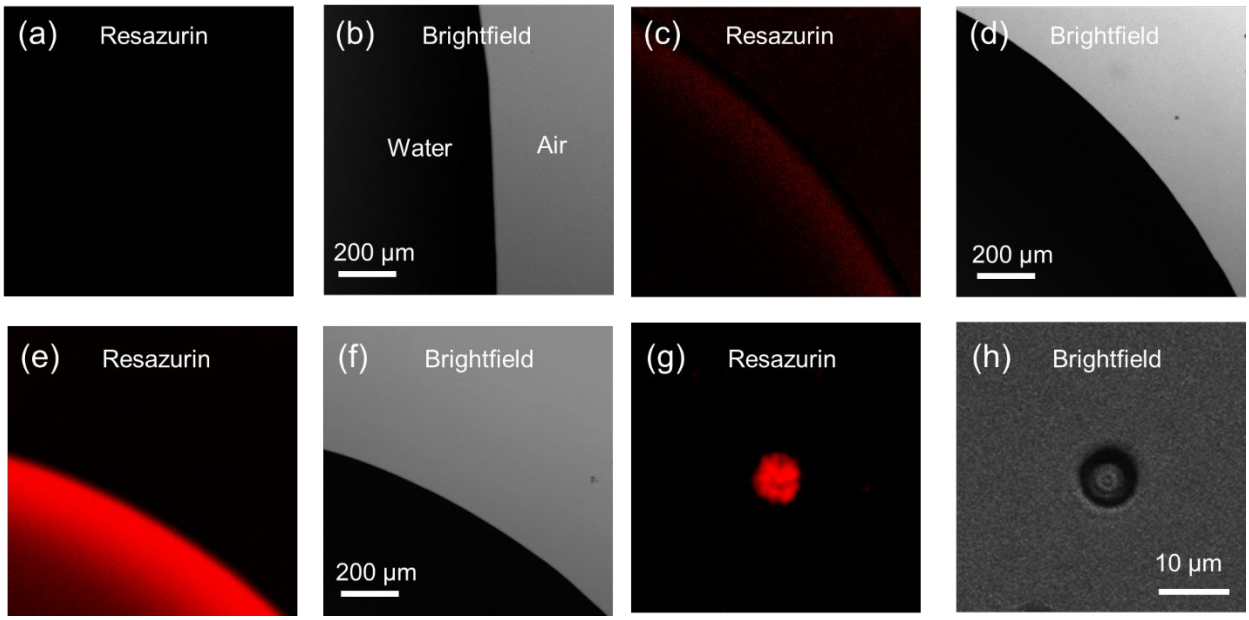

Figure S11. Fluorescence and brightfield images of microdroplets or bulk water containing resazurin. (a-b) Bulk water containing 10-µM resazurin showing no fluorescence. (c-d) Bulk water containing 100-nM resorufin reduced from resazurin by adding nicotinamide adenine dinucleotide (NADH). (e-f) Bulk water containing 10-µM resorufin reduced from resazurin by adding NADH. (g-h) Microdroplet containing 10-µM resazurin. These images confirm that the reduction of resazurin occurred only in microdroplets, not in bulk water. It was also shown that the surface localization is caused by hydrophobicity of resorufin which accumulates at the water-air interface.

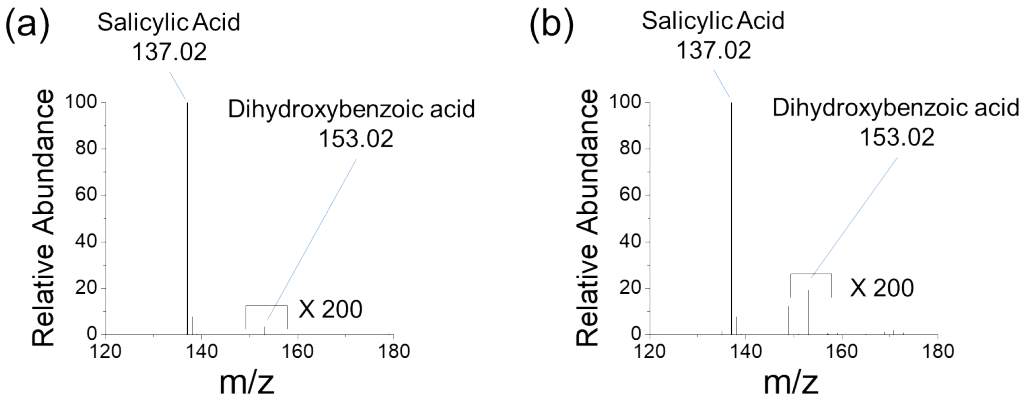

Figure S12. Detection of hydroxyl radicals without or with pyruvate reduction in microdroplets using salicylic acid: (a**)** mass spectrum of spraying 10-µM of salicylic acid without pyruvate, and (b**)** mass spectrum of spraying 10-µM of salicylic acid with 10-nM pyruvate. In both cases, a small peak appeared for dihydroxybenzoic acid corresponding to the capture of the hydroxyl radical by the salicylic acid.

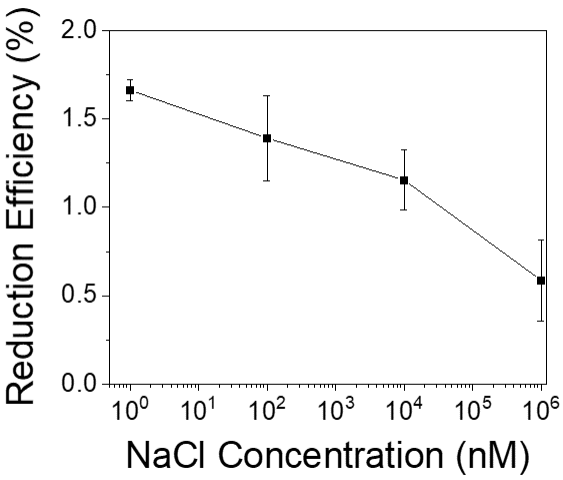

Figure S13. Dependence of reduction efficiency of 100-μM pyruvate on NaCl concentration. The error bars represent one standard deviation from three independent measurements.

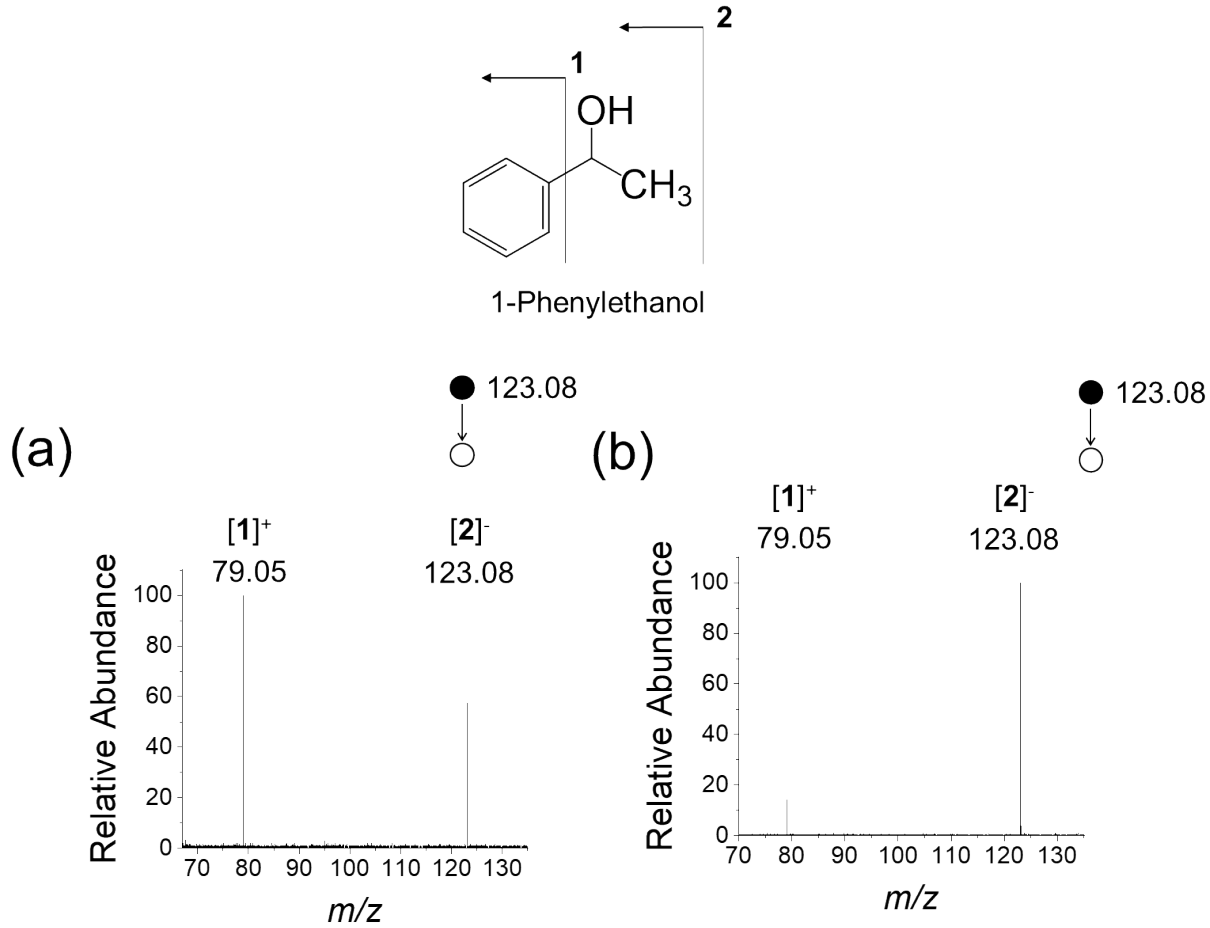

Figure S14. Tandem MS analysis of (a) 1-phenylethanol reduced from acetophenone observed in microdroplets and (b) standard sample of acetophenone.

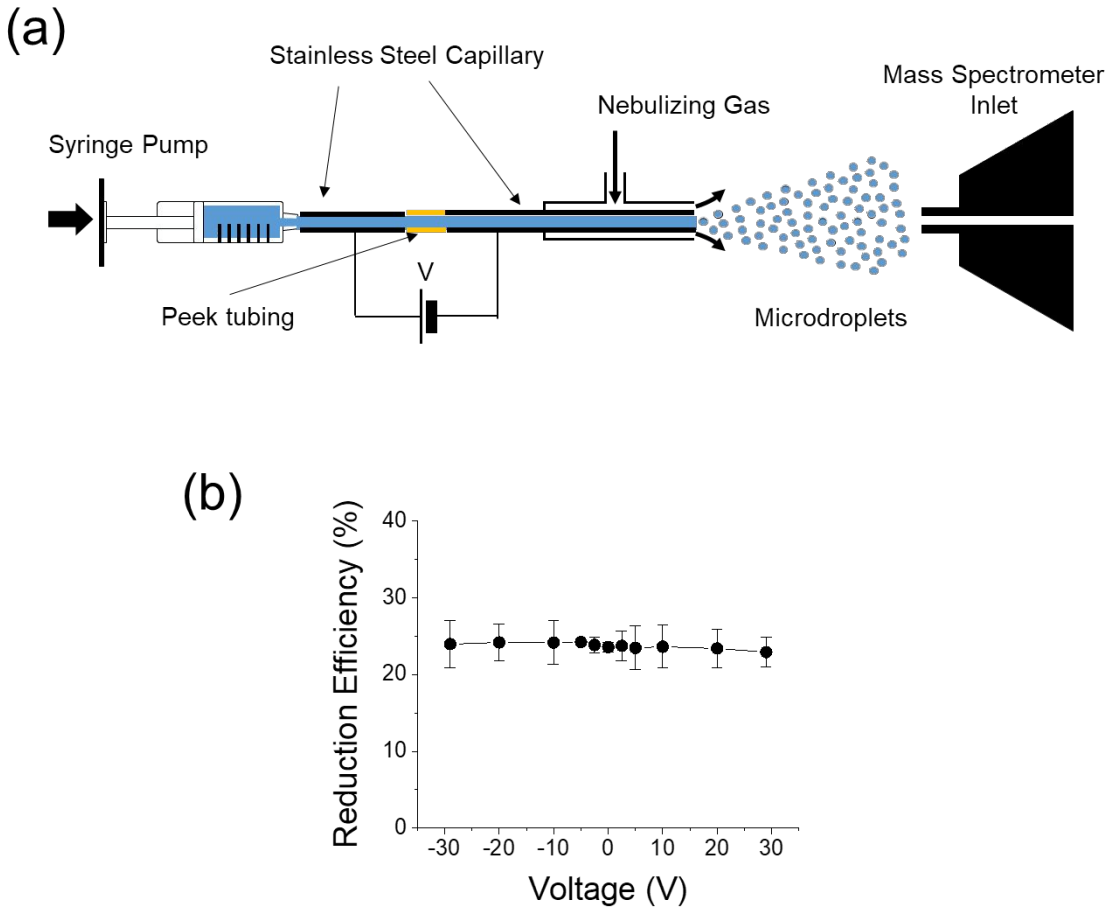

Figure S15. The effect of applied DC, ranging from -29 V to +29 V, between two metal capillaries separated by a polyetheretherketone tubing on reduction efficiency of 1 µM pyruvate: (a) experimental setup, and (b) the reduction efficiency as a function of applied voltage. The error bars represent one standard deviation from three independent measurements.

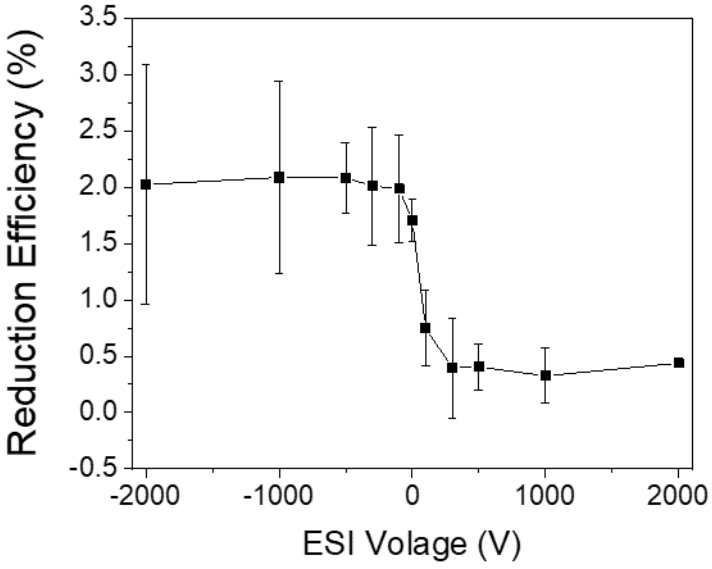

Figure S16. The effect of electrospray ionization (ESI) voltage on the reduction efficiency of 10 μM pyruvate. The error bars represent one standard deviation from three independent measurements.

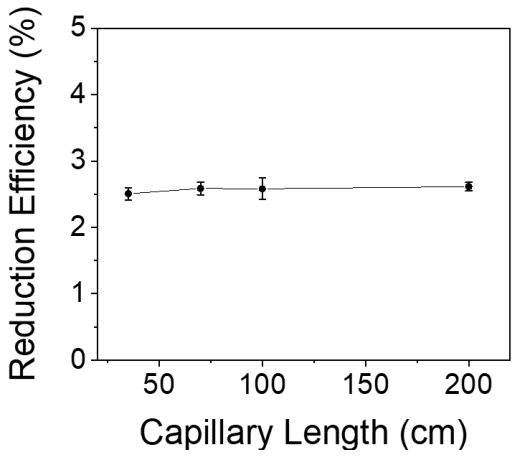

Figure S17. The effect of silica capillary length on reduction efficiency of 1 μM pyruvate. The error bars represent one standard deviation from three independent measurements.

References

1. Liu, C.; Bard, A. J., Electrostatic electrochemistry at insulators. *Nature materials* **2008,** *7* (6), 505.
2. Baumberger, J. P.; Jürgensen, J.; Bardwell, K., The coupled redox potential of the lactate-enzyme-pyruvate system. *The Journal of general physiology* **1933,** *16* (6), 961.
3. Dumitrescu, I.; Anand, R. K.; Fosdick, S. E.; Crooks, R. M., Pressure-driven bipolar electrochemistry. *J. Am. Chem. Soc.* **2011,** *133* (13), 4687-4689.
4. Zilch, L. W.; Maze, J. T.; Smith, J. W.; Ewing, G. E.; Jarrold, M. F., Charge separation in the aerodynamic breakup of micrometer-sized water droplets. *J. Phys. Chem. A* **2008,** *112* (51), 13352-13363.
5. Lee, J. K.; Kim, S.; Nam, H. G.; Zare, R. N., Microdroplet fusion mass spectrometry for fast reaction kinetics. *Proc. Natl. Acad. Sci. U. S. A.* **2015,** *112* (13), 3898-3903.
6. Lee, J. K.; Nam, H. G.; Zare, R. N., Microdroplet fusion mass spectrometry: Accelerated kinetics of acid-induced chlorophyll demetallation. *Q. Rev. Biophys.* **2017,** *50*.
7. Tang, L.; Kebarle, P., Dependence of ion intensity in electrospray mass spectrometry on the concentration of the analytes in the electrosprayed solution. *Anal. Chem.* **1993,** *65* (24), 3654-3668.
8. Winter, B.; Faubel, M.; Hertel, I. V.; Pettenkofer, C.; Bradforth, S. E.; Jagoda-Cwiklik, B.; Cwiklik, L.; Jungwirth, P., Electron binding energies of hydrated H3O+ and OH-: Photoelectron spectroscopy of aqueous acid and base solutions combined with electronic structure calculations. *J. Am. Chem. Soc.* **2006,** *128* (12), 3864-3865.
9. Martins-Costa, M. T.; Anglada, J. M.; Francisco, J. S.; Ruiz-Lopez, M. F., Reactivity of atmospherically relevant small radicals at the air–water interface. *Angew. Chem. Int. Ed.* **2012,** *51* (22), 5413-5417.